# Identifying Critical Factors Influencing Quality of Blood Vessel Information in JPEG Compressed Skin Images

Xiaojie Li
School of Computer Engineering,
Nanyang Technological University,
Block N4, Nanyang Avenue, Singapore 639798
xli16@e.ntu.edu.sg

Adams Wai Kin Kong
School of Computer Engineering,
Nanyang Technological University,
Block N4, Nanyang Avenue, Singapore 639798
adamskong@ntu.edu.sg

***Abstract*—Recent research results demonstrate the potential of using blood vessel patterns for criminal and victim identification. With newly developed methods, blood vessel patterns under human skin are possible to be visualized from evidence images (e.g., child sexual abuse images). However, these images are always taken by consumer cameras and compressed by the JPEG method, which can degrade the blood vessel information seriously. In this paper, an analysis is conducted to find out the critical factors influencing the quality of the blood vessel information. Simulations using different compression ratios are performed on skin images with different resolutions. The results indicate that the quality of blood vessel information is controlled by several low frequency discrete cosine transform (DCT) coefficients in the Y, U and V channels. The findings will be useful for designing algorithms to restore the blood vessel information lost in the JPEG compression process in future research.**

## I. INTRODUCTION

The convenience of the Internet has promoted a mass increase in child sexual abuse images (also known as child pornography). According to a statistic from the Internet Watch Foundation (IWF), there is a huge increase in reports of child sexual abuse images [1]. The number of reports soared from 39,211 in 2012 to 51,186 in 2013 and the rate of rise was 31% [2]. The U.S. Department of Justice reported that there were more than 20 million IP addresses nationwide offering child sexual abuse images and the demand for these images was responsible for the increase in child sexual abuse cases [3]. Criminals in these cases are hard to be identified because they always hide their faces. However, their non-facial skin is always available. This identification problem is not limited to child sexual abuse cases, but also includes masked gunmen, riots and terrorist attacks.

Most of the traditional biometric traits, including face, fingerprint, DNA and palmprint are not applicable to these evidence images. Skin marks, scars, tattoos and androgenic hair patterns definitely give valuable information for identifying the criminals [4-7]. However, none of them is perfect. Not everyone has a unique scar, tattoo, skin mark or androgenic hair pattern on a particular body site. To alleviate this identification problem, researchers developed methods [8-9] to visualize blood vessels in skin images. Their results exposed the potential of using blood vessel patterns for criminal and victim identification. However, most of evidence images in the cases mentioned above are taken by consumer cameras and compressed by the JPEG method [10], which is the most popular image compression method in digital cameras. Blood vessel information in images can be seriously degraded by the JPEG method, which makes the visualization methods not work [8-9]. Note that even in uncompressed images, blood vessel information is weak and is always not observable in unprocessed images. Fig. 1 shows two original forearm images (the first row), their blood vessels given by a visualization method (the second row) [9], their JPEG compressed versions (the third row) and the blood vessels from the JPEG compressed versions (the last row). Fig. 2 shows two original thigh images (the first row), their blood vessels given by the same visualization method (the second row), their JPEG compressed versions (the third row) and the blood vessels from the JPEG compressed versions (the last row). Though the blood vessels from the original images are clear, they are seriously degraded by the JPEG compression method (the last row).

Many methods, including post-filtering methods [11-13], maximum a posteriori (MAP) estimation methods [14-16], wavelet representation based methods [17-18] and methods based on the theory of projection onto convex sets (POCS) [19-20], have been developed to remove blocking artifacts in JPEG compressed images and to enhance their visual quality. However, they are designed for generic images and always smooth the images. They are not suitable for restoring the blood vessel information lost in the JPEG compression process, because they do not extract information from skin image databases. Their smoothing processes may even further weaken the blood vessel information.

978-1-4799-7560-0/15/$31 ©2015 IEEE

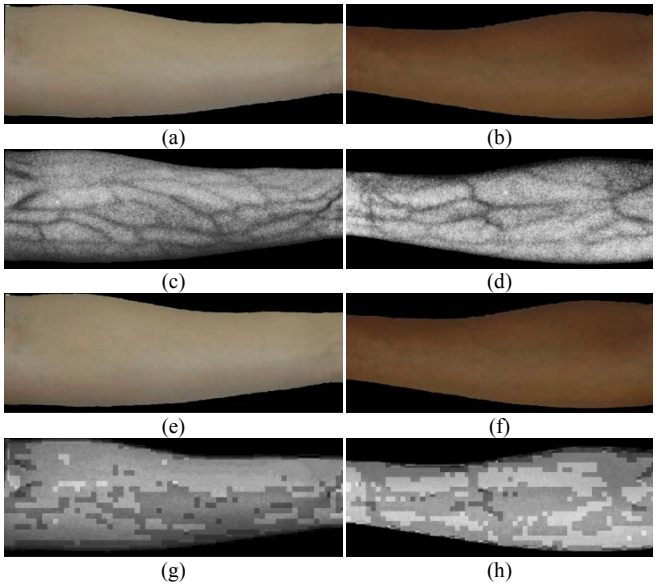

Fig. 1 Two examples of blood vessel images. Each column shows one example. (a)-(b) are the original images. (a) is a left forearm image; (b) is a right forearm image; (c)-(d) show the corresponding blood vessel images from (a)-(b) [9]. (e)-(f) are the JPEG compressed versions of (a)-(b) with a quality factor of 50. (g)-(h) show the blood vessel images from (e)-(f).

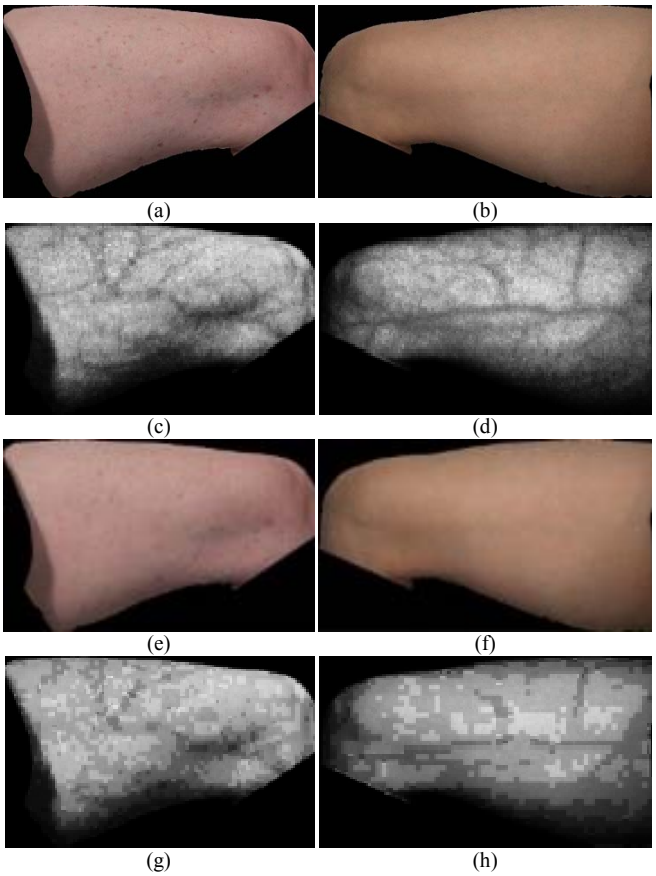

Fig. 2 Two examples of blood vessel images. Each column shows one example. (a)-(b) are the original images. (a) is a left thigh image; (b) is a right thigh image; (c)-(d) show the corresponding blood vessel images from (a)-(b) [9]. (e)-(f) are the JPEG compressed versions of (a)-(b) with a quality factor of 50. (g)-(h) show the blood vessel images from (e)-(f).

The knowledge-based (KB) [21] method and the method proposed in [22] were specially designed for skin image restoration. The KB method was effective to restore skin marks but not for blood vessel information. To finally design an effective algorithm to recover the lost information, the factors which are important to blood vessel quality should be identified. The proposed method in [22] was based on an analysis of skin images. It was neither systematic nor complete. The distribution of the blood vessel information in the YUV channels was neglected and only subjective visual assessment was used to draw the conclusion. In addition, the analysis was performed on several skin images with a fixed resolution and compression factor. The aim of this paper is to systematically identify critical factors influencing quality of blood vessel information in JPEG compressed images. Skin images with different resolutions and different compression factors are tested. The findings in this paper will be useful for designing algorithms to restore the blood vessel information lost in the JPEG compression process in future research.

The rest of this paper is organized as follows. Section II briefly introduces the JPEG method. Section III presents our testing database. Section IV gives the image analysis and the compression test. Section V offers some concluding remarks.

## II. The JPEG Compression Method

Fig. 3(a) gives a schematic diagram of the JPEG compression method. Firstly, images in the RGB color space are transformed to the YUV color space. Then the U and V channels are down-sampled since human vision is less sensitive to information in these two channels. After that, the Y, U and V channels are divided into 8×8 blocks and each block is processed by Discrete Cosine Transform (DCT). The DCT coefficients in each block are arranged in a zigzag order in which a lower order corresponds to a lower frequency. Fig. 3(b) shows the zigzag order. The first element of each block is a DC coefficient and the others are AC coefficients. The quantized DCT (QDCT) coefficients are calculated by,

$$\widetilde{D}_{zj} = \left[D_{zj}/Q_{zj}\right], \tag{1}$$

where $D_{zj}$ is the $j^{th}$ DCT coefficient of a block in $z$ channel; $\widetilde{D}_{zj}$ is the corresponding QDCT coefficient; $Q_{zj}$ is the $j^{th}$ value in a predefined quantization table; $z \in \{\mathrm{Y}, \mathrm{U}, \mathrm{V}\}$ and [ ] is a round operator. According to the JPEG standard, the U and V channels share the same quantization table, which is different from the one for the Y channel. Figs. 3(c) and (d) give two standard quantization tables for generating compressed images with a quality factor of 50, where $Q_y$ is for the Y channel and $Q_{uv}$ is for the U and V channels [10]. It can be seen that most of the values in $Q_{uv}$ are larger than the corresponding ones in $Q_y$. When the values are larger, the compression ratio is higher and the image quality is worse. Thus, the image quality degradation is more serious in the U and V channels than that in the Y channel. After the quantization operation, the QDCT coefficients are encoded using a lossless coding scheme to get the final compressed

image. Information loss takes place in the down-sampling process and blockwise quantization, which degrade not only image quality but also blood vessel visibility.

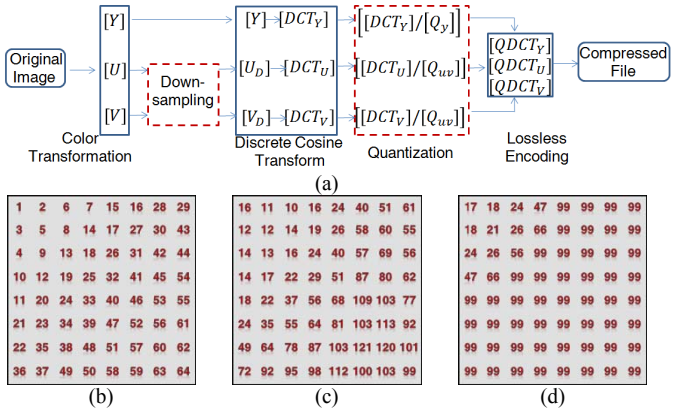


Fig. 3 Introduction to the JPEG method. (a) is an illustration of the JPEG compression method. (b) is the zigzag order. (c) is the quantization table $Q_y$ for the Y channel with a quality factor of 50 and (d) is the quantization table $Q_{uv}$ for the U and V channels with a quality factor of 50.

## III. A Skin Image Database

Table I summarizes the skin image database used in this study. It includes four limb image datasets: a left forearm dataset, a right forearm dataset, a left thigh dataset and a right thigh dataset. The four datasets were respectively collected from 239, 250, 230 and 228 subjects. Each subject was taken two images in two sessions with a time difference of 11 days. Totally, there are 1,894 images in the database. Fig. 4 gives raw sample images in the database. The figure shows that the image collection configuration is not strictly restricted. For example, the poses of the subjects were different. The illustration and the background were also changed. In addition, the race and age of the subjects were different. The raw images were first saved in the JPEG format with a high quality factor so that there was no obvious compression artifact. Then, the limbs were extracted from the raw images and aligned for this study. To remove the compression effect, the images were resized. The preprocessed images were referred to as original (uncompressed) images in this study. Images shown in Figs. 1-2 are preprocessed images. The database is publically available [23]. It should be emphasized that high resolution images are always collected in cases of child sexual abuse and other sexual offenses.

TABLE I. A SUMMARY OF THE DATABASE

| Datasets | Abbreviation | Number of images |
|---|---|---|
| The 1st session of the left forearm dataset | LF1 | 239 |
| The 2nd session of the left forearm dataset | LF2 | 239 |
| The 1st session of the right forearm dataset | RF1 | 250 |
| The 2nd session of the right forearm dataset | RF2 | 250 |
| The 1st session of the left thigh dataset | LT1 | 230 |
| The 2nd session of the left thigh dataset | LT2 | 230 |
| The 1st session of the right thigh dataset | RT1 | 228 |
| The 2nd session of the right thigh dataset | RT2 | 228 |

To analyze compression impacts on blood vessels in images with different resolutions, skin images in the testing database are downscaled to generate a lower resolution image database. The original database is denoted as DB1 and the lower resolution one is denoted as DB2. The average image sizes of these two databases are shown in Table II. The images in DB2 are compressed to a quality factor of 75. Figs. 5-6 show the lower resolution version of the images in Figs. 1-2. Figs. 5(a) and (b) are two uncompressed forearm images, and Figs. 5(c) and (d) give the corresponding blood vessel images. Figs. 5(e) and (f) show the JPEG compressed images of Figs. 5(a) and (b) with a quality factor of 75. Figs. 5(g) and (h) show the corresponding blood vessel images. Figs. 6(a) and (b) are two uncompressed thigh images and Figs. 6(c) and (d) give the corresponding blood vessel images. Figs. 6(e) and (f) are the compressed images with a quality factor of 75, and Figs. 6(g) and (h) show the corresponding blood vessel images.


Fig. 4 Raw sample images from the database. (a) is from the forearm datasets and (b) is from the thigh datasets.

TABLE II. THE AVERAGE IMAGE SIZE

| Datasets | DB1 | | DB2 | |
|---|---|---|---|---|
| | *Length (pixels)* | *Width (pixels)* | *Length (pixels)* | *Width (pixels)* |
| LF1 | 960 | 396 | 480 | 186 |
| LF2 | 955 | 390 | 480 | 184 |
| RF1 | 1017 | 368 | 480 | 162 |
| RF2 | 1019 | 374 | 480 | 163 |
| LT1 | 1124 | 649 | 512 | 289 |
| LT2 | 1129 | 653 | 512 | 287 |
| RT1 | 1082 | 628 | 512 | 291 |
| RT2 | 1103 | 612 | 512 | 281 |

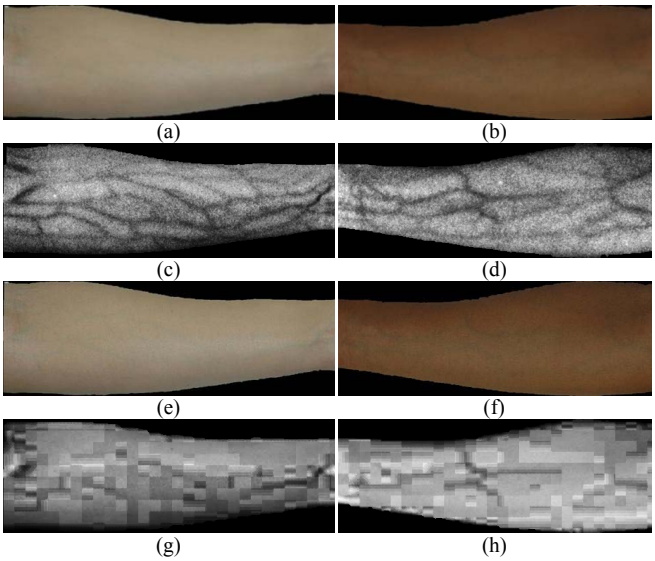


Fig. 5 The lower resolution version of Figs. 1(a) and (b). (a)-(b) are the original images. (c)-(d) are the corresponding blood vessel images from (a)-(b) [9]. (e)-(f) are the JPEG compressed versions of (a)-(b) with a quality factor of 75. (g)-(h) are the blood vessel images from (e)-(f).

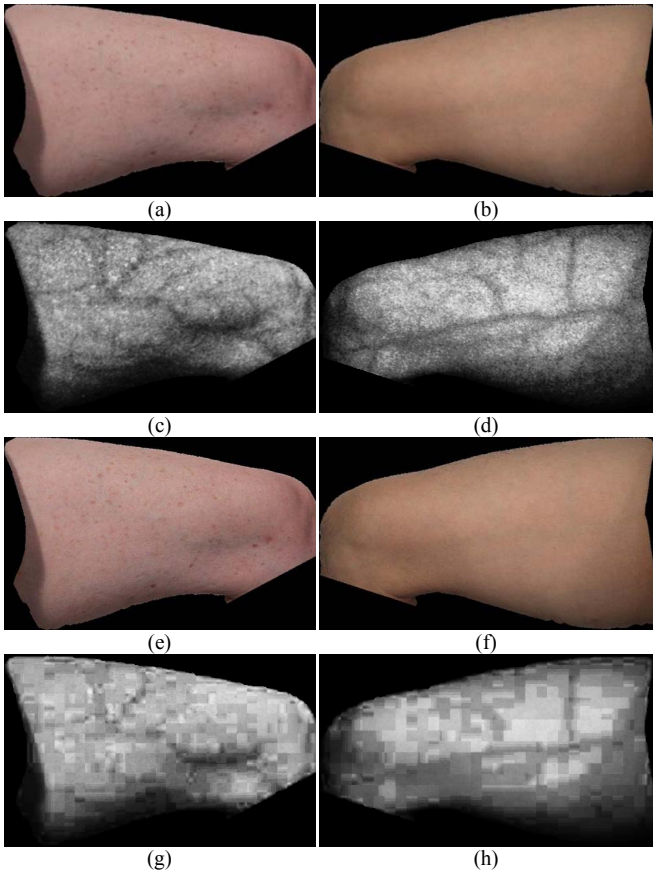

Fig. 6 The lower resolution version of Figs. 2(a) and (b). (a)-(b) are the original images. (c)-(d) are the corresponding blood vessel images from (a)-(b) [9]. (e)-(f) are the JPEG compressed versions of (a)-(b) with a quality factor of 75. (g)-(h) are the blood vessel images from (e)-(f).

## IV. A Statistical Analysis And A Compression Test

Since the JPEG compression method processes images in the YUV color space, intuitively, restoration algorithms should operate in this space. Thus, it is necessary to know how blood vessel information distributes in the luminance channel (the Y channel) and the chrominance channels (the U and V channels). To perform this analysis, the visualization and matching methods described in [9] are used to evaluate blood vessel information in different channels. In the first test, the information in the chrominance channels is removed, but the information in the luminance channel is retained. In the second test, the information in the chrominance channels is retained, but the information in the luminance channel is removed. By comparing the matching results in these two tests, it can be known which channels contain more blood vessel information. Eq. 2 is the transformation equation from the YUV color space to the RGB color space [24] in a range of [0, 255],

$$\begin{bmatrix} R \\ G \\ B \end{bmatrix} = \begin{bmatrix} 1.164 & 0 & 1.596 \\ 1.164 & -0.392 & -0.813 \\ 1.164 & 2.017 & 0 \end{bmatrix} \begin{bmatrix} Y - 16 \\ U - 128 \\ V - 128 \end{bmatrix}. \quad (2)$$

If both the U and V values are 128, Eq. 2 can be rewritten as,

$$\begin{bmatrix} R \\ G \\ B \end{bmatrix} = \begin{bmatrix} 1.164 & 0 & 1.596 \\ 1.164 & -0.392 & -0.813 \\ 1.164 & 2.017 & 0 \end{bmatrix} \begin{bmatrix} Y - 16 \\ 0 \\ 0 \end{bmatrix}. \quad (3)$$

Eq. 3 indicates that the information in the U and V channels are eliminated and only the Y channel contributes to the RGB values. In other words, if skin images are processed by Eq. 3, the resultant blood vessels will only have the Y channel information. Thus, in the first test, images in the two databases are first converted into the YUV space. Then the pixel values in the U and V channels are set to 128 and the images are converted back to the RGB space. It is worth to mention that the blood vessel visualization method used in this analysis and the latter experiments takes RGB images as inputs [9]. Similarly, in the second test, the pixel values in the Y channel are set to 16, but the pixel values in the U and V channels are retained.

After producing the testing images, the blood vessel visualization method is applied. Figs. 7-8 show, respectively, the results from the images given in Figs. 1 (a)-(b) and Figs. 2 (a)-(b). Only a few blood vessels from the Y channel (Figs. 7(a) and 8(a)) are observable, while the blood vessels from the U and V channels (Figs. 7(b) and 8(b)) are close to the ones from the original images (Figs. 1(c)-(d) and Figs. 2(c)-(d)), except for some details. It indicates that all the three channels contain blood vessel information, but the Y channel carries less information than the U and V channels. The same conclusion can be drawn from the lower resolution images which are shown in Figs. 9-10. To determine the quality of the blood vessel information in different channels, instead of subjective visual observation, a three-step blood vessel matching method [9] measuring dissimilarity between two blood vessel patterns is used. Cumulative match characteristic (CMC) curves are employed as a performance index. In this analysis, the original images in DB1 and DB2 collected in the first session are, respectively, matched with their JPEG compressed versions with quality factors of 50 and 75 as references. The images with only Y channel information and the images with only U and V channel information are also matched with the original images. In these tests, the original images are used as gallery sets and the other images are used as probe sets. Figs. 11-12 show the CMC curves and indicate three important points. The JPEG compression method seriously deteriorates the blood vessel quality. The images with only the U and V channel information provide much higher matching accuracy than those with only the Y channel information. The U and V channels contain much more information than the Y channel, but they all contain blood vessel information, which agrees with the previous visual comparison. The images in the second session are also matched. The results indicate the same three important points. Thus, their CMC curves are not given in here. Cross session matching (e.g. the 1st vs. the 2nd sessions) is not performed because the aim of these tests is to study the distributions of blood vessel information in the three channels, but not to evaluate the visualization and matching algorithms.

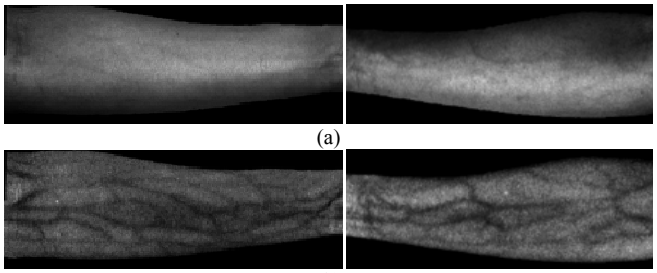

Fig. 7 Resultant images of the image analysis. (a) is the results from the analysis on the Y channel and (b) is the results from the analysis on the U and V channels.

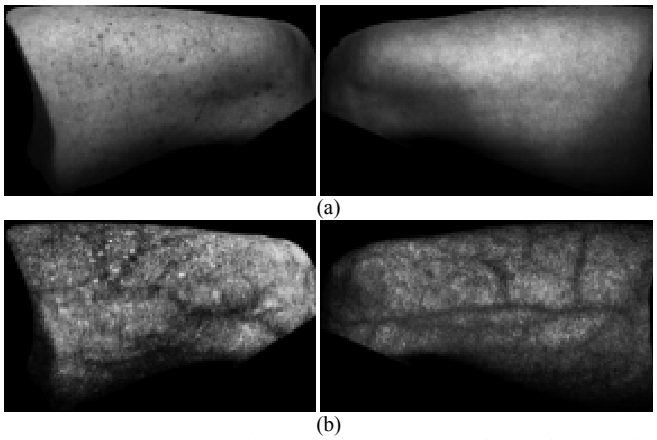

Fig. 8 Resultant images of the image analysis. (a) is the results from the analysis on the Y channel and (b) is the results from the analysis on the U and V channels.

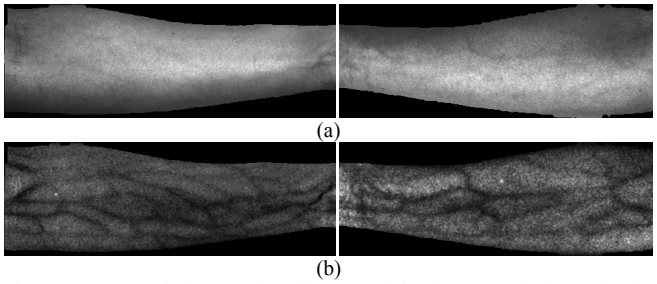

Fig. 9 Lower resolution resultant images of the image analysis. (a) is the results from the analysis on the Y channel and (b) is the results from the analysis on the U and V channels.

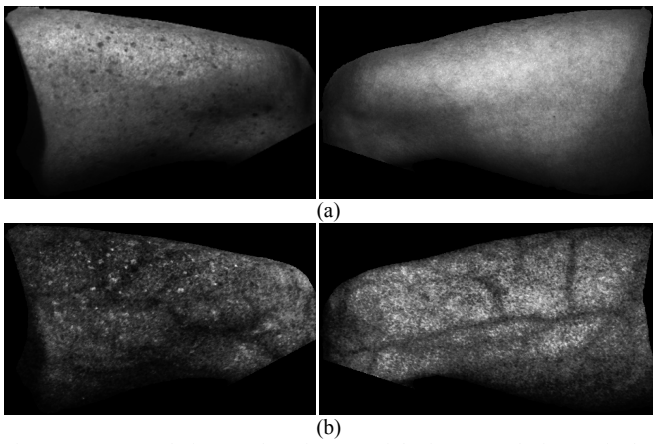

Fig. 10 Lower resolution resultant images of the image analysis. (a) is the results from the analysis on the Y channel and (b) is the results from the analysis on the U and V channels.

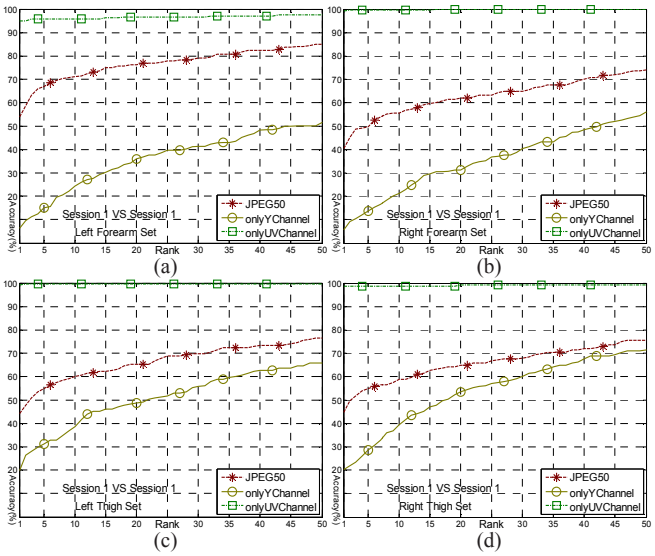


Fig. 11 The matching results of DB1 from the image analysis. (a)-(d) are CMC curves from LF1, RF1, LT1 and RT1, respectively. In the legends, JPEG50 means JPEG compressed images with a quality factor of 50; onlyYChannel means the images with only the Y channel information and onlyUVChannel means the images with only the U and V channel information.

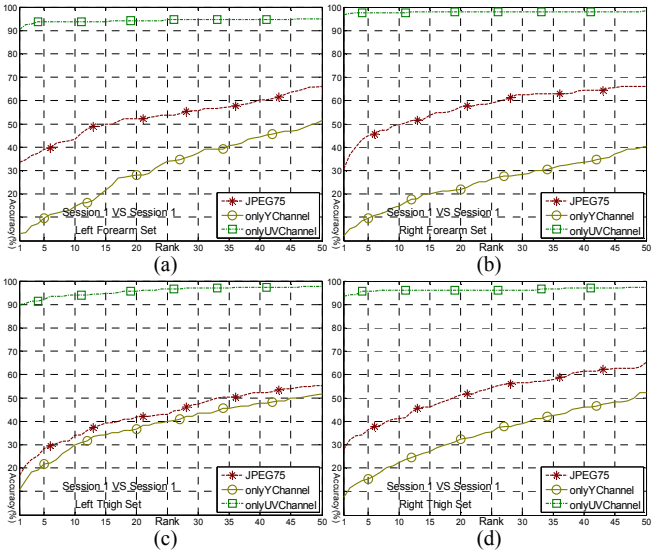


Fig. 12 The matching results of DB2 from the image analysis. (a)-(d) are CMC curves from LF1, RF1, LT1 and RT1, respectively. In the legends, JPEG75 means JPEG compressed images with a quality factor of 75; onlyYChannel means the images with only the Y channel information and onlyUVChannel means the images with only the U and V channel information.

A compression test is further conducted to identify how the lossy operations (which are the down-sampling operation and the quantization operation highlighted by the red dash rectangles in Fig. 3(a)) in the JPEG compression method degrade the quality of blood vessel information. In this test, the down-sampling operation and the quantization operation are examined separately. Fig. 13 shows the compression processes in the test. The compression process given in Fig. 13(a) only applies the down-sampling procedure to the U and V channels and the original Y channel is preserved, so that its effect can be observed. Fig. 13(b) shows that the Y, U and V channels are quantized with the modified quantization

tables $Q_{yi}$ and $Q_{uvi}$ after the down-sampling operation in the U and V channels. This compression process is designed to figure out how the quantization operation affects the quality of blood vessel information. To further identify critical DCT coefficients, the standard quantization tables are modified to generate three pairs of quantization tables. Fig. 14 gives the quantization tables $Q_{yi}$ for the Y channel and $Q_{uvi}$ for the U and V channels, where $i \in \{1,2,3\}$. They are modified from $Q_y$ and $Q_{uv}$ in Figs. 3(c) and (d) which are used to generate compressed images with a quality factor of 50. Comparing with the original $Q_y$ and $Q_{uv}$, it can be noted that several original values are modified to '1's, which means that the corresponding DCT coefficients are only processed by the round function. In each pair of $Q_{yi}$ and $Q_{uvi}$, the number and the position of '1' are same. The DCT coefficients are organized in a zigzag order (Fig. 3(b)) according to their frequency. The modified values in the quantization tables are in the same order. The same modification scheme is applied to the original quantization tables of a quality factor of 75 to generate three pairs of quantization tables.

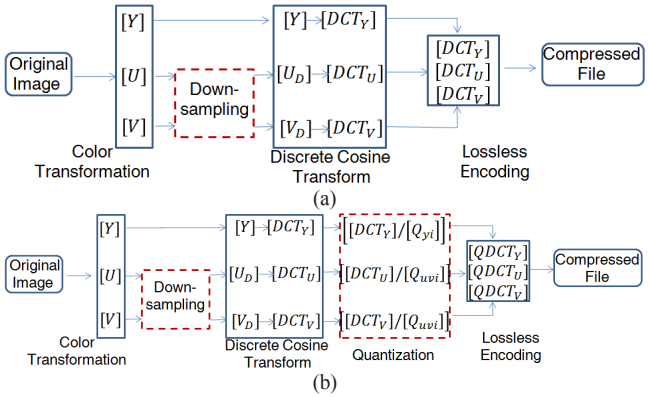


Fig. 13 The processes of the compression test. (a) is to evaluate the down-sampling procedure in the U and V channels. (b) is to evaluate the quantization operation in the Y, U and V channels.

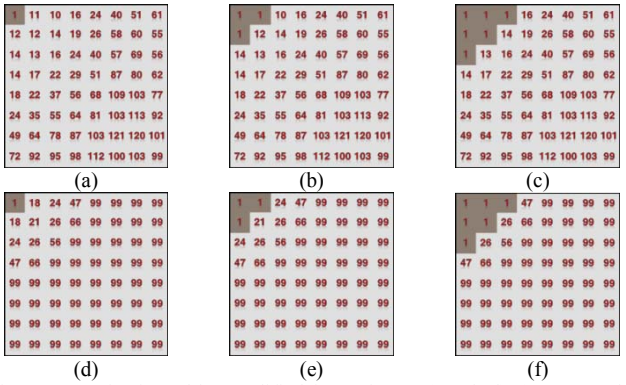


Fig. 14 Quantization tables modified from Figs. 3(c) and (d). (a)-(c) are the quantization tables for the Y channel, which are respectively denoted as $Q_{y1}$, $Q_{y2}$ and $Q_{y3}$, and (d)-(f) are the quantization tables for the U and V channels, which are respectively denoted as $Q_{uv1}$, $Q_{uv2}$ and $Q_{uv3}$.

The two databases are used in this test and the two compression processes in Fig. 13 are applied to the images. Figs. 15-16 give four testing results of DB1 from the compression process in Fig. 13(a). Figs. 15(a) and 16(a) show the resultant color images, whose original images are given in Figs. 1(a)-(b) and Figs. 2(a)-(b). Figs. 15(b) and 16(b) show the corresponding blood vessel images. Figs. 15(b) and 16(b) indicate that the blood vessels obtained from the compressed images are similar to those from the original images (Figs. 1(c)-(d) and Figs. 2(c)-(d)). There is no obvious degradation comparing to Figs. 1(c)-(d) and Figs. 2(c)-(d). Figs. 17-18(a), (c) and (e) show the results generated by the compression process in Fig. 13(b). They are corresponding to the three modified quantization table pairs, $\{Q_{y1}, Q_{uv1}\}$, $\{Q_{y2}, Q_{uv2}\}$ and $\{Q_{y3}, Q_{uv3}\}$ in Fig. 14. Figs. 17-18 (b), (d) and (f) are the corresponding blood vessel images. The results indicate that the more '1's in the quantization tables, the clearer blood vessel images are. There are obvious blocking artifacts in Figs. 17(b) and 18(b), which are generated by the quantization tables $Q_{y1}$ and $Q_{uv1}$. The blocking artifacts are weaker in the results from the quantization tables $Q_{y2}$ and $Q_{uv2}$, which are shown in Figs. 17(d) and 18(d). The results (Figs. 17(f) and 18(f)) generated by the quantization tables $Q_{y3}$ and $Q_{uv3}$ are very close to the blood vessel images (Figs. 1(c)-(d) and Figs. 2(c)-(d)) generated from the original images. The same compression processes in Fig. 13 are applied to the images in DB2. The three pairs of quantization tables generated from the quantization tables of a quality factor of 75 are used in the compression process in Fig. 13(b). The compressed results have the same visual effects. Thus, the results are not given in here.

To objectively compare the quality of blood vessels generated by the compression test, blood vessel patterns are extracted from the compressed images and matched with the blood vessel patterns from the original images [9]. As with the previous tests, the original images in the first session are used as gallery sets and the other images are used as probe sets. The matching results are given in Figs. 19-20. The blood vessel images from the JPEG compressed images are also matched with the original images as references. The results show that the down-sampling operation in the U and V channels does not affect the quality of the blood vessels. The results also show that the first six DCT coefficients in the Y, U and V channels contain critical blood vessel information for matching. The images in the second session are also matched. The results give the same observation and therefore, their CMC curves are not given in here. This study points out that the quantization operation degrades the quality of blood vessel information and the first six coefficients in the three channels are critical.

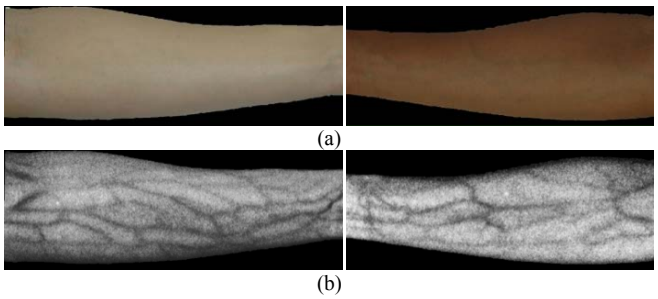


Fig. 15 (a) is the resultant color images from the compression process given in Fig. 13(a) and their original images are given in Figs. 1(a)-(b). (b) shows the corresponding blood vessel images from the compressed images.

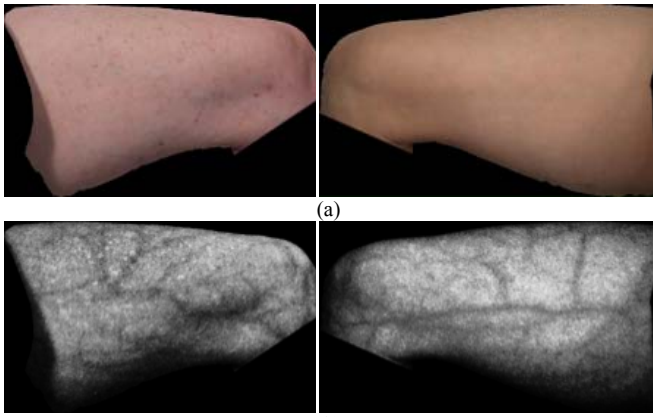

Fig. 16 (a) is the resultant color images from the compression process given in Fig. 13(a) and their original images are given in Figs. 2(a)-(b). (b) shows the corresponding blood vessel images from the compressed images.

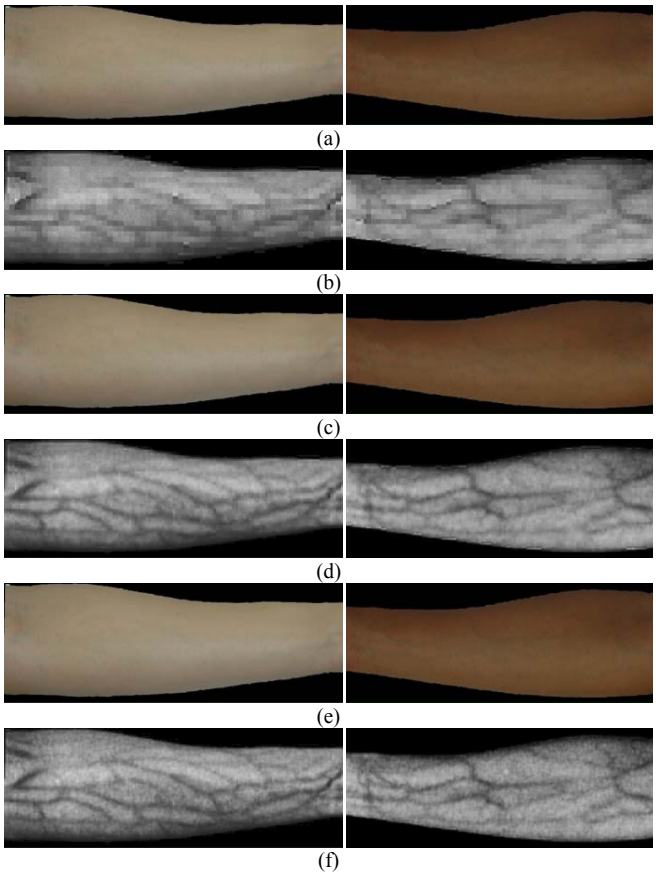

Fig. 17 Results from the compression process given in Fig. 13(b). (a) is generated by $\{Q_{y1}, Q_{uv1}\}$, (c) is generated by $\{Q_{y2}, Q_{uv2}\}$ and (e) is generated by $\{Q_{y3}, Q_{uv3}\}$. (b), (d) and (f) are respectively blood vessel images.

## V. Conclusion

The potential of using blood vessel information in color images for criminal and victim identification has been exposed recently. However, the JPEG compression method, which is the most popular image compression method installed in digital cameras, can seriously degrade its quality. In this paper, an analysis is performed to identify the factors that influence the quality of blood vessel information. JPEG compressed skin images with different resolutions and different compression ratios are analyzed. The results indicate that the low frequency DCT coefficients in all the channels play a vital role. The findings will be useful for developing algorithms to recover the blood vessel information lost in the JPEG compression process in future research.


## Acknowledgment

This work is partially supported by the Ministry of Education, Singapore through Academic Research Fund Tier 2, MOE2012-T2-1-024.


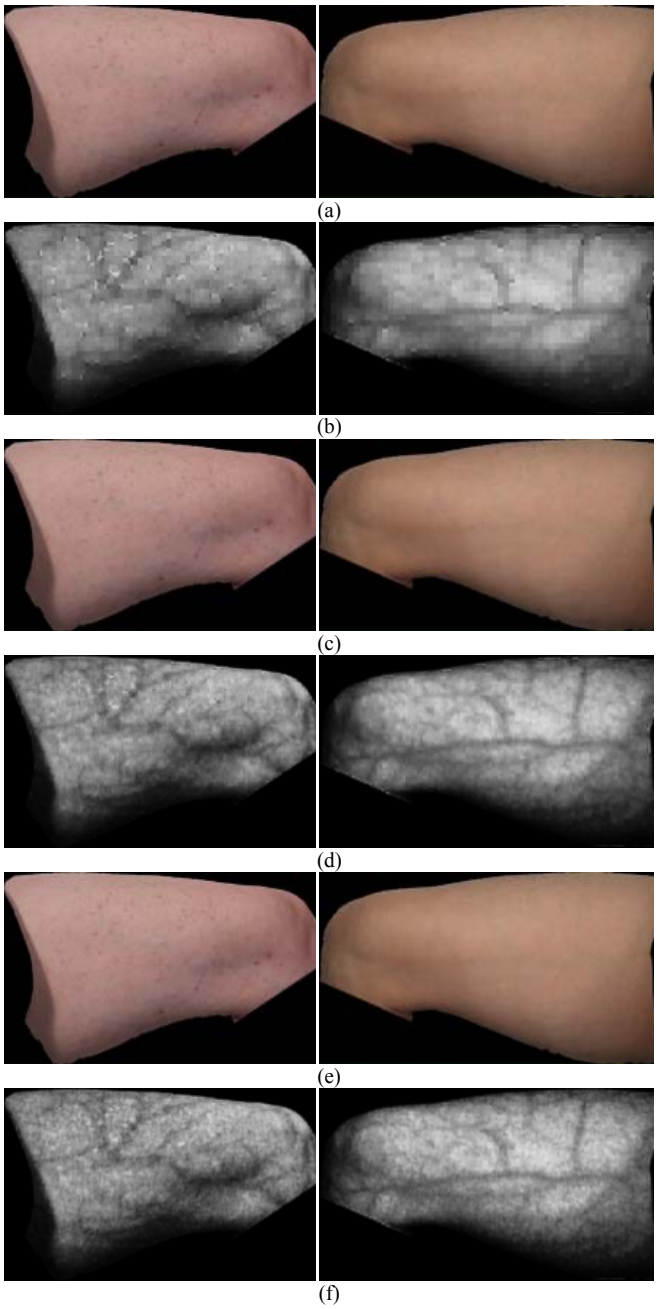

Fig. 18 Results from the compression process given in Fig. 13(b). (a) is generated by $\{Q_{y1}, Q_{uv1}\}$, (c) is generated by $\{Q_{y2}, Q_{uv2}\}$ and (e) is generated by $\{Q_{y3}, Q_{uv3}\}$. (b), (d) and (f) are respectively blood vessel images.

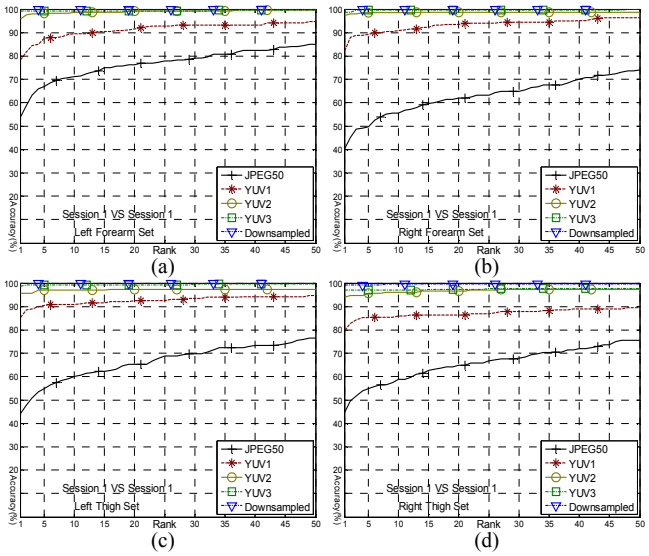


Fig. 19 The matching results of DB1 from the compression test. (a)-(d) are CMC curves from LF1, RF1, LT1 and RT1, respectively. In the legends, JPEG50 means the JPEG compressed images with a quality factor of 50; Downsampled means that only the down-sampling operation is applied to the U and V channels but the original Y channel is preserved and YUV$i$ means that the Y, U and V channels are quantized by $\{Q_{yi}, Q_{uvi}\}$, where $i \in \{1, 2, 3\}$.

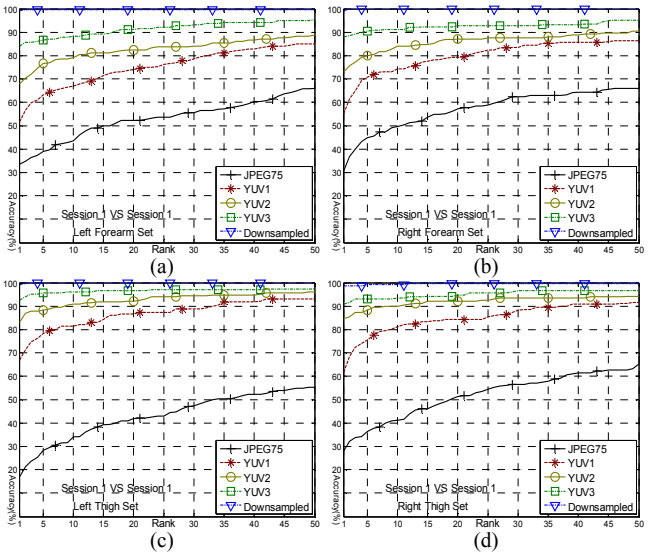


Fig. 20 The matching results of DB2 from the compression test. (a)-(d) are CMC curves from LF1, RF1, LT1 and RT1, respectively. In the legends, JPEG75 means the JPEG compressed images with a quality factor of 75; Downsampled means that only the down-sampling operation is applied to the U and V channels but the original Y channel is preserved and YUV$i$ means that the Y, U and V channels are quantized by the three modified quantization tables, respectively.

## REFERENCES


[1] http://www.thetimes.co.uk/tto/technology/internet/article40495-80.ece.

[2] http://www.heraldscotland.com/news/crime-courts/pictures-of-child-sex-abuse-are-hidden-in-uk-sites.23881400.

[3] U. S. D. o. Justice, "National strategy for child exploitation prevention and interdiction: a report to congress," 2010.

[4] A. Nurhudatiana, A. W. K. Kong, K. Matinpour, S.-Y. Cho and N. Craft, "Fundamental statistics of relatively permanent pigmented or vascular skin marks for criminal and victim identification," in *IJCB*, pp. 1-6, 2011.

[5] A. Nurhudatiana, A. W. K. Kong, K. Matinpour, D. Chon, L. Altieri, S.-Y. Cho and N. Craft, "The individuality of relatively permanent pigmented or vascular skin marks (RPPVSM) in independently and uniformly distributed patterns," *IEEE TIFS,* vol. 8, no. 6, pp. 998-1012, 2013.

[6] H. Su and A. W. K. Kong, "A study on low resolution androgenic hair patterns for criminal and victim identification," *IEEE TIFS,* vol. 9, no. 3-4, pp. 666-680, 2014.

[7] J.-E. Lee, A. K. Jain and R. Jin, "Scars, marks and tattoos (SMT): Soft biometric for suspect and victim identification," in *BSYM*, pp. 1-8, 2008.

[8] C. Tang, A. W. K. Kong and N. Craft, "Uncovering vein patterns from color skin images for forensic analysis," in *CVPR*, pp. 665-672, 2011.

[9] H. Zhang, C. Tang, A. W. K. Kong and N. Craft, "Matching vein patterns from color images for forensic investigation," in *BTAS*, pp. 77-84, 2012.

[10] G. K. Wallace, "The JPEG still picture compression standard," *ACM Commun.,* vol. 34, no. 4, pp. 30-44, 1991.

[11] H. C. Reeve III and J. S. Lim, "Reduction of blocking effects in image coding," *Optical Engineering,* vol. 23, no. 1, pp. 34-37, 1984.

[12] Y. Luo and R. K. Ward, "Removing the blocking artifacts of block-based DCT compressed images," *IEEE TIP,* vol. 12, no. 7, pp. 838-842, 2003.

[13] A. Foi, V. Katkovnik and K. Egiazarian, "Pointwise shape-adaptive DCT for high-quality denoising and deblocking of grayscale and color images," *IEEE TIP,* vol. 16, no. 5, pp. 1395-1411, 2007.

[14] D. Sun and W.-K. Cham, "Postprocessing of low bit-rate block DCT coded images based on a fields of experts prior," *IEEE TIP,* vol. 16, no. 11, pp. 2743-2751, 2007.

[15] H. Noda and M. Niimi, "Local MAP estimation for quality improvement of compressed color images," *PR,* vol. 44, no. 4, pp. 788-793, 2011.

[16] X. Zhang, R. Xiong, X. Fan, S. Ma and W. Gao, "Compression artifact reduction by overlapped-block transform coefficient estimation with block similarity," *IEEE TIP,* vol. 22, no. 12, pp. 4613-4626, 2013.

[17] Z. Xiong, M. T. Orchard and Y.-Q. Zhang, "A deblocking algorithm for JPEG compressed images using overcomplete wavelet representations," *IEEE TCSVT,* vol. 7, no. 2, pp. 433-437, 1997.

[18] A.-C. Liew and H. Yan, "Blocking artifacts suppression in block-coded images using overcomplete wavelet representation," *IEEE TCSVT,* vol. 14, no. 4, pp. 450-461, 2004.

[19] C. Weerasinghe, A.-C. Liew and H. Yan, "Artifact reduction in compressed images based on region homogeneity constraints using the projection onto convex sets algorithm," *IEEE TCSVT,* vol. 12, no. 10, pp. 891-897, 2002.

[20] J. Park, D.-C. Park, R. J. Marks and M. A. El-Sharkawi, "Recovery of image blocks using the method of alternating projections," *IEEE TIP,* vol. 14, no. 4, pp. 461-474, 2005.

[21] C. Tang, A. W. K. Kong and N. Craft, "Using a knowledge-based approach to remove blocking artifacts in skin images for forensic analysis," *IEEE TIFS,* vol. 6, no. 3, pp. 1038-1049, 2011.

[22] X. Li and A. W. K. Kong, "Restoring blood vessel patterns from JPEG compressed skin images for forensic analysis," in *WIFS*, pp. 19-24, 2013.

[23] NTU Forensic Skin Database, http://forensics.sce.ntu.edu.sg/.

[24] C. A. Poynton, "A technical introduction to digital video," John Wiley & Sons, Inc., pp. 175-176, 1996.